

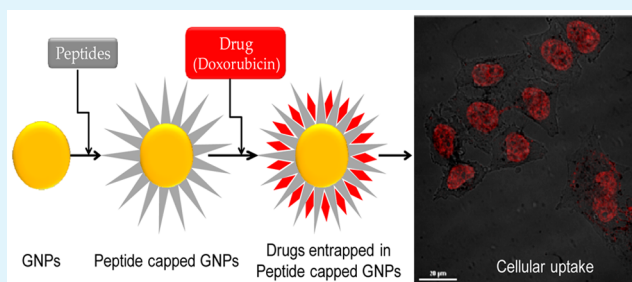
Non-natural Amino Acids Containing Peptide-Capped Gold Nanoparticles for Drug Delivery Application

Shaheena Parween, Ashraf Ali, and Virander S. Chauhan*

International Centre for Genetic Engineering and Biotechnology, New Delhi

ABSTRACT: Peptide-based capping agents for gold nanoparticles (GNPs) are possible alternatives for capping and derivatizing GNPs, but suffer from a major disadvantage of sensitivity toward non specific proteases, which may limit their in vivo utility. Using non-natural analogs of natural α -amino acids offer an attractive alternate strategy to circumvent this potential bottleneck in realizing full potential of peptide based capping agents for GNPs for biological applications. Here, we have designed and developed pentapeptides containing non-natural amino acid (α,β -dehydrophenylalanine and α -aminoisobutyric acid) as capping agents for GNPs. All these peptides were able to efficiently cap GNPs and peptide induced aggregation was not observed. Peptide capped GNPs showed minimal cytotoxicity to mammalian cell lines (HeLa and L929) as well as mice spleenocytes. They encapsulated small drug like molecules and peptide capped GNPs entrapping drugs were more efficient in killing HeLa cells compared to the free drug. Therefore, these non-natural amino acid containing peptide-capped GNPs may be further developed as alternate drug delivery vehicles.

KEYWORDS: peptide, gold nanoparticles, drug delivery, non-natural amino acids



1. INTRODUCTION

Gold nanoparticles (GNPs) have found wide applications in the field of biomedical sciences because of their unique optical properties and amenability to functionalization with biomolecules as well as drugs.^{1–6} Stability under physiological conditions is a prerequisite for such in vivo applications.^{6–8} Because of high surface energy, GNPs tend to aggregate in ionic solutions that limit their applications. To overcome this limitation, GNPs are coated with organic molecules, which reduces the surface energy of GNPs and thus provide increased solubility in ionic solution.^{9,10} Various thiol ligands with hydrophilic end groups as well as polymeric capping agents have been used previously to increase stability of GNPs.^{2,11–13} Thiol ligands form self-assembling monolayers (SAM) on GNPs and are considered better as the size change in nanoparticles after capping is minimum and provide ease of functionalization.^{14,15} Various self-assembling ligands have been described such as alkanethiols and peptides.^{9,14–16}

Amino terminus cysteine-containing peptides have been shown as efficient capping agents for various metal nanoparticles.^{17,18} The minimal requirements for a peptide to act as a robust capping agent for GNPs have been investigated previously.¹⁹ A cysteine at the N-terminus of peptide is required for metal binding, a core of hydrophobic amino acids for packing and polar amino-acids at the C-terminus of peptide to provide solubility in physiological environments. Moreover, these peptides can prevent aggregation of GNPs induced by salts and are amenable for easy functionalization for biomolecular recognition.^{19–21} Although peptide-based capping agents offer a myriad of potential toward solubility and functionalization of nanoparticles,²² yet their comparative instability toward proteases may be a key concern

in realizing their full potential in biomedical applications.^{23–25} In fact, a recent study has shown that almost one-third of the peptides derived from biological sources are susceptible to degradation by Cathepsin L protease.²⁴ Particularly, pentapeptide CALNN, which was recently used as capping agent for GNPs, was cleaved by Cathepsin L.²⁴ Such vulnerability to biological proteases greatly limits the use of peptide-capped GNPs for biological applications. However, using non-natural amino acids containing peptides could be an attractive alternative to the natural α -amino acid containing peptides, as they are known to be relatively stable to the action of biological proteases.^{23,26,27}

Here, we have designed, synthesized and investigated the capping efficiency of GNPs by a series of pentapeptides incorporating non-natural amino acids (α,β -dehydrophenylalanine, Δ Phe; and α -aminoisobutyric acid, Aib). The phenylalanine analog Δ Phe, contains a double bond between C_α and C_β atoms, whereas Aib is alanine analog with an additional methyl group at C_α . Introduction of Δ Phe and Aib in peptide sequences is well-known to provide them increased resistance toward enzymatic degradation.^{23,28–30} Peptide capped GNPs were further characterized by UV–vis spectroscopy, dynamic light scattering (DLS), electron microscopy (EM), and agarose gel electrophoresis. Cellular uptake and cytotoxicity of peptide capped GNPs on mammalian cells was also studied. We further investigated the ability of these peptide capped GNPs to encapsulate and release various drugs to mammalian cells.

Received: September 30, 2012

Accepted: June 14, 2013

Published: June 14, 2013

2. MATERIALS AND METHODS

2.1. Synthesis and Characterization of GNPs. The synthesis of GNPs was carried out according to Turkevich et al. as described previously.^{31,32} Briefly, 100 mL of 1 mM hydroauric chloride (HAuCl₄) was reduced with sodium citrate (10 mL, 38.8 mM) under refluxing condition. The reaction mixture was stirred for 30 min to obtain a dark red solution. After the pH of the solution was adjusted to 7.0 with aqueous NaOH, the solution was filtered and stored at room temperature. To determine the molarity and size of GNPs, we carried out UV–visible spectroscopy in 400–800 nm range using 1 cm path length cuvette. Dynamic light scattering (DLS) and transmission electron microscope (TEM) was used to check the size distribution of GNPs.

2.2. Synthesis and Characterization of Peptides. All peptides were synthesized using standard Fluorenylmethyloxycarbonyl (Fmoc) chemistry on Wang's resin (0.75 mmol/g) as described previously.²⁹ N,N'-Diisopropylcarbodiimide (DIPCDI) and N-hydroxybenzotriazole (HOBt) were used as coupling agents and Fmoc was removed using 20% piperidine in Dimethylformamide (DMF). Amino acid coupling and Fmoc deprotection were examined by Kaiser test.³³ ΔPhe was incorporated into peptides using Fmoc-X-ΔPhe azalactone dipeptide block and coupling was done overnight in DMF.^{29,34} After the completion of peptide synthesis and subsequent Fmoc removal, the resin was washed extensively with DMF, dichloromethane (DCM), and methanol and dried in a vacuum-desiccator. The cleavage of peptides from the resin was carried out using Reagent R (Trifluoroacetic acid (TFA):thioanisole: ethanedithiol (EDT):anisole, 90:5:3:2) for 3 h at room temperature. After resin removal by filtration, the peptide was precipitated from cleavage mixture by adding cold anhydrous diethyl ether. Further, the precipitate was washed with ether and lyophilized from acetic acid:water (10%, v/v). The peptides were purified by preparative reverse phase HPLC on C18 column using linear gradient of acetonitrile–water (5–75% acetonitrile, 0.1%TFA/water, 0.1% TFA) as described earlier.³⁵ The purified peptides were verified by electrospray ionization mass spectrometry.

2.3. Capping of GNPs with Peptide and Characterization of the Capped GNPs. Peptide-capped GNPs were obtained by mixing GNPs and peptides(10:1, v/v) in phosphate buffer as described previously with slight modifications.¹⁹ Peptide-capped GNPs were characterized by UV–visible spectrometry, DLS, gel electrophoresis and TEM. To check salt-induced aggregation, we calculated the aggregation parameter (AP) using UV–vis spectrometry, which is defined as $AP = (A - A_0)/A_0$, where A is the integrated absorbance (600–700 nm) of the sample at different concentration of salt and A_0 is the integrated absorbance (600–700 nm) of the starting GNPs.¹⁹ For AP determination, were incubated samples for 30 min before taking absorbance.

2.3.1. Agarose Gel Electrophoresis. Electrophoresis of GNPs and peptide capped GNPs was carried out using 1% (w/v) agarose gel electrophoresis as described previously.³⁶ Equal volume of samples and Ficol (20%) was mixed for loading on to gels and electrophoresis was done at 70 V/cm for 30 min using 1XTAE as running buffer. After the separation, peptide-capped GNPs were detected as red band.

2.3.2. Electron Microscopy. Peptide capped GNPs were prepared as described above for observation under transmission electron microscope (TEM). Samples were adsorbed on carbon coated Formvar film, negative stained with 1% uranyl acetate and visualized by TEM (Tecnai 12 TWIN, FEI Netherlands) at 120 kV. Size of GNPs was determined by analyzing TEM images using Analysis III software.

2.3.3. Circular Dichroism (CD). CD spectra of peptide and peptide capped GNPs were recorded under conditions described previously with slight modification.³⁷ A quartz cuvette of 0.5 cm path length was used and spectra were taken in 10 mM phosphate buffer with a response time of 4 s (scan speed 100 nm/min). Five scans were averaged for the spectra analysis.

2.3.4. Fourier Transform Infrared (FTIR) Spectroscopy. Solution state (D₂O, cells of 0.01 mm optical path and CaF₂ windows) IR spectra were collected on a Perkin-Elmer model BX FTIR spectrometer. Peptide capped GNP samples were prepared in D₂O and spotted on a CaF₂ window. 100 spectra were collected (resolution of 4 cm⁻¹), averaged and smoothed with a smoothing length of 20 for analysis.

The FTIR spectra were smoothed with smoothing length of 20. *Spectrum* (Perkin-Elmer) was used for the spectra processing.

2.4. Drug-Loading Studies. Drug loading experiment was done according to the method described previously with slight modification.³⁸ Briefly, three drug molecules (chloroquine, mitoxantrone(Mito) and doxorubicin(Dox)) were mixed with 1 nM CALNN/CFΔFNN capped GNPs in 1:5 volume ratios resulting in final drug concentration of 2×10^{-6} M in solution. The mixture of drug and GNPs were incubated overnight at 4 °C and then centrifuged at 15000 rpm for 1 h. Supernatant was removed and used for the determination of the free test molecules concentration spectrophotometrically. The percentage loading was calculated using the following formula³⁹

$$\% \text{loading} = \left[\frac{\text{(total amount of drug added)} - \text{(amount of drug in supernatant)}}{\text{total amount of drug added}} \right] \times 100$$

2.5. Cytotoxicity of Peptide-Capped GNPs. Two mammalian cell lines (HeLa and L929) and mice splenocytes were selected to evaluate cytotoxicity of peptide-capped GNPs. The experiment was carried out using method described previously.⁴⁰ Briefly, mammalian cells(1×10^4 cells/well) and splenocytes(1×10^5 cells/well) were cultured in triplicate in 96 well plates. The cells were incubated with graded concentration of peptide capped GNPs for 24–72 h. Twenty microliters of MTT stock solution (5 mg/mL in PBS) was added per well. After 4 h incubation, formazan crystals were dissolved with 200 μL of DMSO after removing the media. The microplate reader (Molecular Devices) was used to measure the absorbance of each well at 570 nm. The relative cell viability compared to control cells with media (without nanoparticles) was calculated by $[A]_{\text{test}}/[A]_{\text{control}}$. 0.06% of polyethylene imine (PEI), CALNN, and CFΔFNN were used as controls.

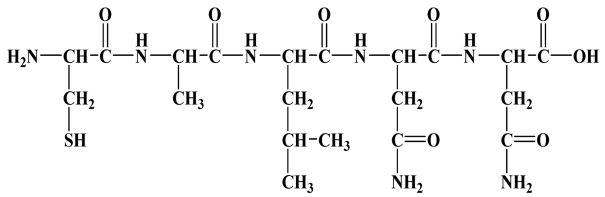
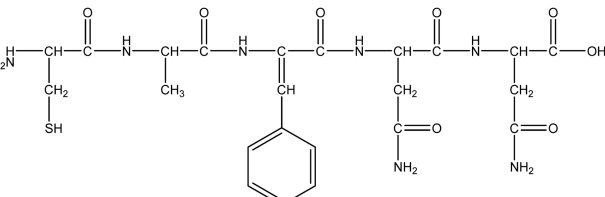
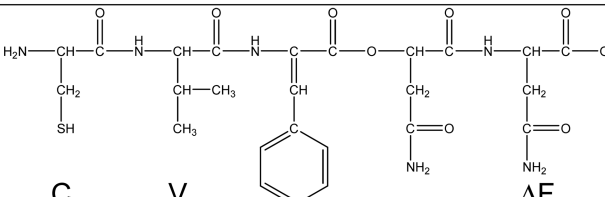
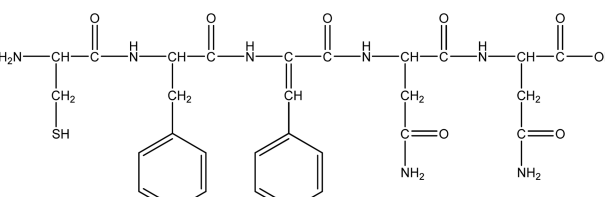
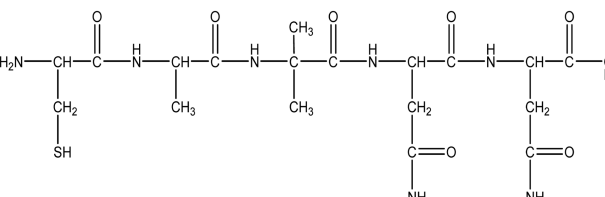
Two cell lines, HeLa and L929, were used for testing the effective delivery of two drugs; doxorubicin (Dox) and mitoxantrone (Mito) by peptide-capped GNPs. Free Dox/Mito and peptide-Dox/Mito were used as control and cell viability was checked with MTT assay as described above.

2.6. Cellular Uptake. HeLa and L929 cell lines were maintained in RPMI with 10% fetal bovine serum (FBS), glutamine (2 mM), penicillin (50 U/mL) and streptomycin (0.05 g/mL). For confocal microscopy, HeLa cells were removed using a trypsin(0.25%) ethylenediaminetetraacetic acid (EDTA) solution, and seeded on glass coverslips, further grown at 37 °C with 5% CO₂ to attain 60% confluency. Cells were then incubated with Dox (5 μM) and Dox (5 μM) + CFΔFNN-GNP (5 nM) for 1 h. Dox (5 μM)+CFΔFNN(5 μM) and CFΔFNN-GNP (5 nM) were taken as controls. After incubation was complete, cells were washed using phosphate-buffered saline (PBS, 3 times) and fixed with 4% paraformaldehyde. Then, the coverslips were mounted on a microscope slide with in DAPI containing antifade mounting media and examined using a NikonA1 confocal laser scanning microscope with a 60× objective. Rodamine and phase contrast channels were used for imaging cells.

Further cellular uptake of Dox with peptide capped GNPs was carried out using flow cytometry as described previously.⁴¹ Briefly, HeLa and L929 cells were added in 6-well plates (1×10^5 cells per well) in RPMI. Dox(5 μM) alone or mixed with CALNN(5 μM), CFΔFNN (5 μM), CALNN-GNP(5 nM), and CFΔFNN-GNP(5 nM) were incubated with cells for 1 h at 37 °C. A well containing cells and CFΔFNN-GNP (5 nM) alone was used as negative control. After incubation, cells were detached using trypsin/EDTA solution and washed twice with PBS to remove surface associated drugs. Cells were taken in flow cytometry buffer and flow cytometry (FACSCalibur-Becton Dickinson) was done using FL2 channel. CellQuest software was used to represent mean fluorescence signal collected for 10 000. All experiments were carried out in triplicate.

2.7. Proteolytic Stability Assays. The peptides (CALNN and CFΔFNN) were incubated with a nonspecific protease, proteinase K taken at a ratio of 100:1 (molar ratio) in 10 mM Tris of pH 8 and incubated at 37 °C. After 1 h, the samples were aliquoted and analyzed by reversed-phase HPLC on C18 column (Phenomenex: 5 μm, i.d. 250 × 4.6 mm) using linear gradient acetonitrile–water (5–95%) with

Table 1. Amino Acid Sequence, Structure, and Characterization of Designed Peptides

Peptide sequence and structure	Mass (Calculated)	Mass (Observed)
 <p>C A L N N</p>	533.6	534.3
 <p>C A ΔF N N</p>	565.6	565.2
 <p>N C V ΔF N</p>	593.6	593.2
 <p>C F ΔF N N</p>	641.7	642.3
 <p>C A U N N</p>	505.5	506

1 mL per min flow rate. Relative decrease in the peak area of the peptide was used to compare proteolytic degradation.

3. RESULTS AND DISCUSSION

3.1. Peptide Design, Synthesis, and Characterization. The peptide selection was based on the pentapeptide sequence

CALNN, where cysteine at the *N*-terminus contains thiol for binding GNPs. The nonpolar side chains of hydrophobic core(AL) are capable of self-assembling into well-packed layer excluding water. Apart from these interactions of hydrophobic residues, hydrogen bonding of amide backbone causes efficient packing of the peptides on the GNP surface yielding large surface

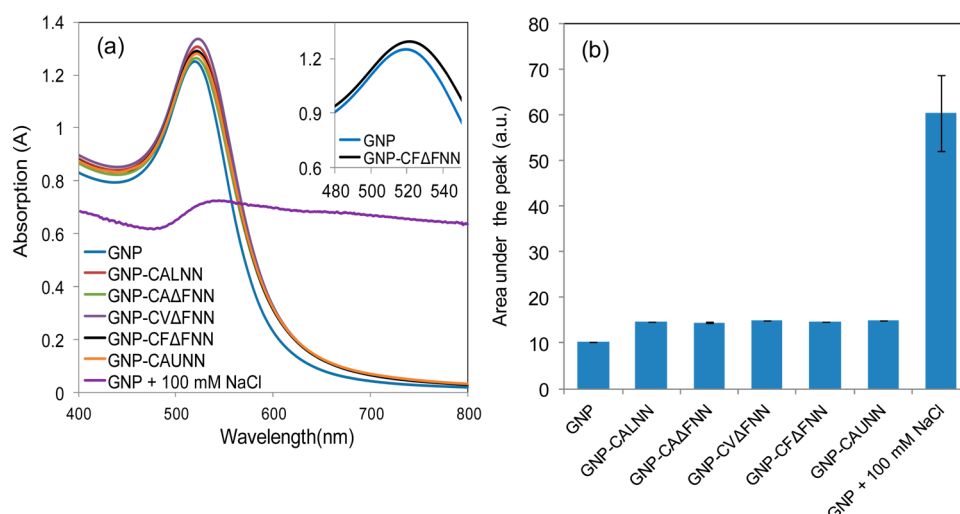


Figure 1. (a) Spectra of uncapped, CALNN, CAΔFNN, CVΔFNN, CAUNN, CFΔFNN-capped GNPs and GNPs treated with 100 mM NaCl. Inset: Spectra of uncapped (blue) and CFΔFNN capped GNPs (black) at high magnification. (b) Area under the SPR peak in the wavelength range 600–700 nm (mean \pm SD; $n = 2$).

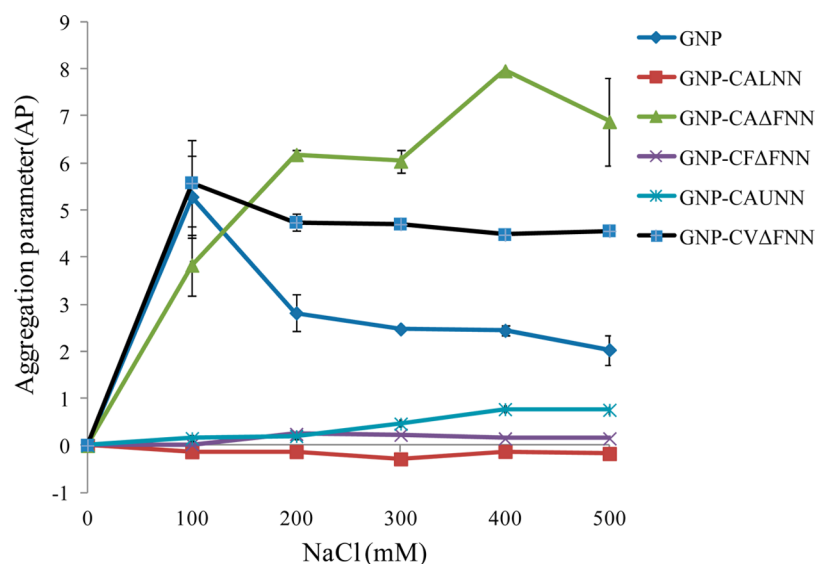


Figure 2. Aggregation parameter of uncapped, CALNN, CAΔFNN, CVΔFNN, CAUNN, and CFΔFNN-capped GNPs with increasing concentration of NaCl.

charge densities.¹⁹ We kept cysteine and terminal Asn constant in all our peptides as these are required for GNP conjugation and provide a polar character for efficient dispersion in solution, respectively. We replaced the internal hydrophobic residues (Ala-Leu) with hydrophobic non-natural amino acids and hypothesized that these noncoded amino acids should provide both well packed self-assembled monolayers on GNP surface as well as stability against proteases. Dipeptides containing ΔPhe have been shown to self-assemble into well organized nanostructures and are protease stable.^{30,37} On the basis of this background, we synthesized three peptides CAΔFNN, CVΔFNN, and CFΔFNN containing ΔPhe and CAUNN, where Leu was replaced by small hydrophobic noncoded Aib(U) residue. Peptides were synthesized by standard Fmoc chemistry on Wangs resin, purified to homogeneity by HPLC and further their identity was confirmed by mass spectrometry (Table 1).

3.2. Synthesis, Capping of GNPs, and Characterization. GNPs were synthesized by citrate reduction of hydroauric chloride as described in material and methods and analyzed by

UV–visible spectroscopy. The characteristic broad absorption band due to surface plasmon effect of GNPs was observed with its peak at 519 nm (Figure 1). CALNN was chosen as template and as a control for stabilization of the GNPs, as this peptide successfully stabilizes GNPs in higher electrolyte concentration.¹⁹ As shown in Figure 1a, after the addition of these peptides to the GNP solution, there is an immediate shift of 1 to 3 nm in the surface plasmon peak (λ_{SPR}). λ_{SPR} of GNPs was shifted from 519 nm upon capping with CAΔFNN; to 521 by CFΔFNN and CAUNN while to 522 nm upon capping by CALNN and CVΔFNN. This peak shift is due to adsorption of the peptide onto the GNP surface leading to changes in local dielectric permittivity around the GNPs and is a qualitative measure of capping.⁴² Also, the area under the curve in the wavelength range 600–700 nm of GNPs (10) and all four peptide capped GNPs (~ 15) were comparable suggesting no peptide induced aggregation of GNPs. Here, GNPs treated with 100 mM NaCl was used as positive control and the area under the curve observed was 60 (Figure 1b).

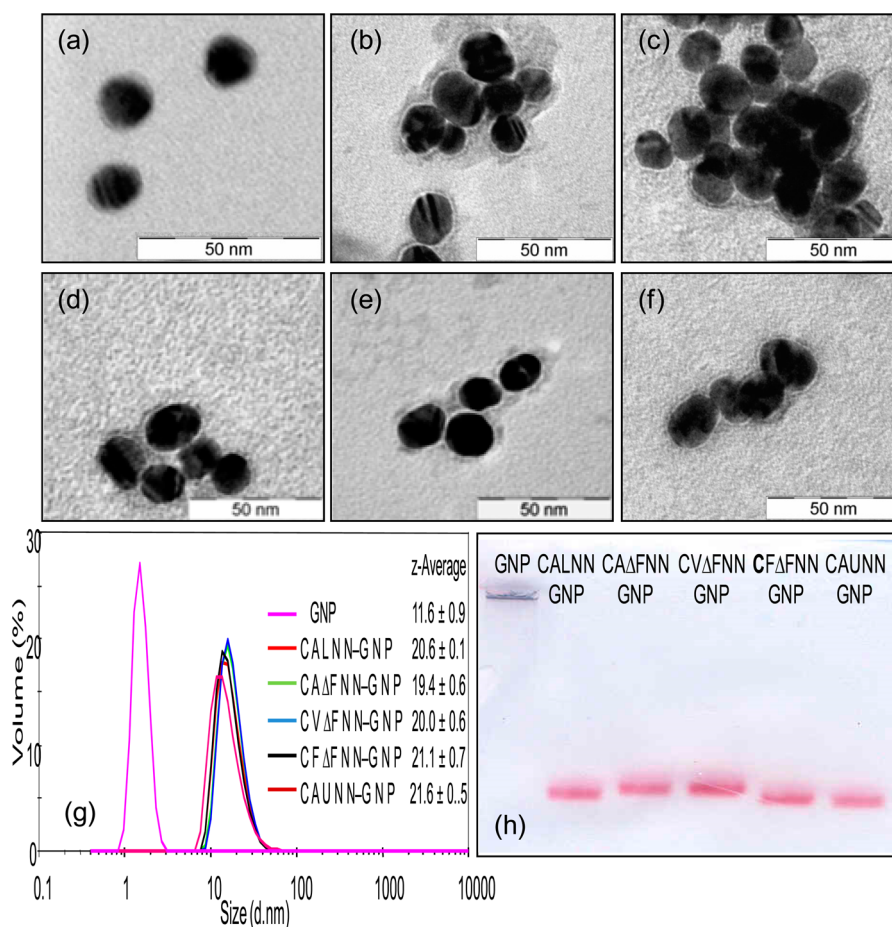


Figure 3. TEM of (a) GNP, (b) CALNN-GNPs, (c) CAΔFNN-GNPs, (d) CVΔFNN-GNPs, (e) CFΔFNN-GNPs, (f) CAUNN-GNPs, and (g) DLS and (h) 1% Agarose gel electrophoresis of GNP and peptide-capped GNPs. Samples b–f were stained with 1% uranyl acetate before imaging, whereas sample a is unstained GNPs. Scale bars = 50 nm.

Nanoparticle stabilization in high ionic condition is crucial for use in biomedical application and in physiologically relevant solutions. Intact surface plasmon band of GNPs demonstrate its stability in the physiological ionic condition. Increase of absorption at 600–700 nm is used to monitor aggregation of nanoparticles.¹⁹ A new absorption band at longer wavelengths is formed after aggregation of GNPs which is caused by dipole coupling between the plasmons of aggregating nanoparticles. Aggregation Parameter (AP) as described in materials and methods was used to test capping efficiency of CAΔFNN, CVΔFNN, CFΔFNN, and CAUNN against salt-induced aggregation of GNPs, where CALNN-capped GNPs were taken as control. In agreement with earlier studies,¹⁹ CALNN-GNPs were stable, even up to 500 mM of NaCl with negligible aggregation parameter (Figure 2). For CAΔFNN-GNP, aggregation parameter increased rapidly from 3.83 to 6.88 with 100 mM to 500 mM salt concentration; however CVΔFNN-GNP aggregated immediately and showed AP of 5.58 at 100 mM NaCl. On the other hand CAUNN capped GNPs were relatively stable at higher salt concentrations with AP of 0.75 at 500 mM NaCl concentration. This is in agreement with the results of Levy and co-workers where incorporation of bulkier amino acids led to aggregation while small hydrophobic amino acids were well tolerated.¹⁹ Interestingly, CFΔFNN containing bulkier amino acids provided stability to GNPs even at a very high salt concentration of 500 mM with AP of 0.15; which was comparable to that of CALNN-GNP (Figure 2). This enhanced stability of CFΔFNN, compared to the other peptides

tested, could be attributed to high propensity of Phe-ΔPhe to self-assemble and enhanced packing provided by aromatic residues.³⁰ CFΔFNN capped GNPs were most stable, so we did all of our further studies with CFΔFNN-capped GNPs.

To check the capping of peptides onto GNPs, we further characterized peptide capped GNPs by TEM, DLS and gel electrophoresis. As shown in Figure 3b–e, TEM images clearly show ~2 nm uniform layer of peptides on GNPs whereas no layer is observed in naked GNPs (Figure 3a). Furthermore, capping of peptides on GNPs led to ~9 nm increase of hydrodynamic diameter (z-average) of GNPs as seen by dynamic light scattering (DLS) (Figure 3g). In addition, peptide capping onto GNPs was also checked by gel electrophoresis (Figure 3h). Because of local precipitation of naked GNPs in TAE running buffer, it did not come out of wells. Peptide capping onto GNPs were able to avoid electrostatic interaction, providing stability to GNPs. Peptide-capped GNPs migrated in agarose gel as red bands. These results qualitatively show the successful peptide capping on to GNPs and further providing them stability.

Conformational changes in the CFΔFNN peptides upon forming monolayers upon GNPs were assessed by circular dichroism (CD) and Fourier transform infrared (FTIR) spectroscopy. The CD spectrum of CFΔFNN in the far-UV region showed positive bands at 222 nm of $n-\pi^*$ transition and at 203 nm of $\pi-\pi^*$ transition, suggestive of a turn like structure (Figure 4a). However, the CD spectrum in the near-UV region showed negative CD at 245 nm (Phe absorption) and at 270 nm

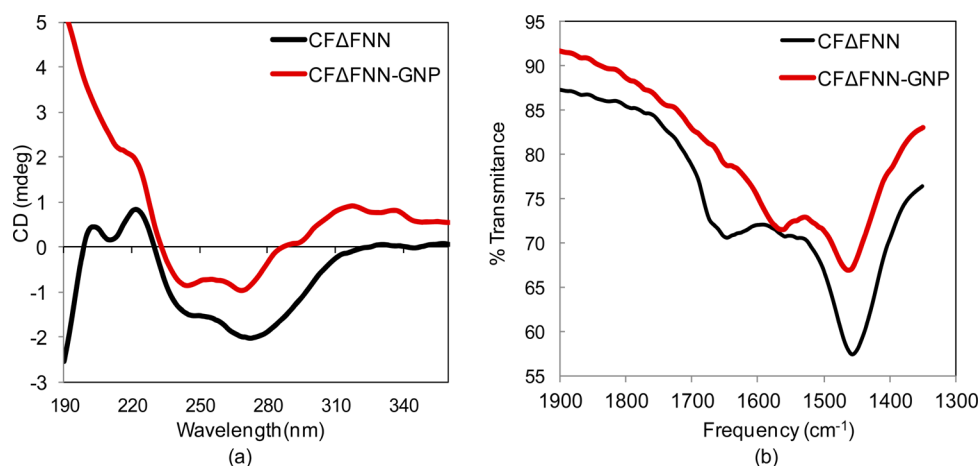


Figure 4. Conformational changes in the CF Δ FNN peptides upon capping on GNPs. (a) CD spectra and (b) FTIR spectra of CF Δ FNN (black lines) and CF Δ FNN-GNPs (red lines).

(Δ Phe absorption). CF Δ FNN-GNP showed a 5 nm shift in near-UV region suggesting different packing arrangement of Δ Phe residue on GNP surface relative to the free CF Δ FNN. This was further verified by the change in π - π^* transition at 203 nm after capping onto GNPs (Figure 4a). In the FTIR spectrum of CF Δ FNN, amide I and amide II peaks were observed at 1647 and 1558 cm^{-1} respectively (Figure 4b). In the case of GNP-capped CF Δ FNN, amide I and amide II peaks were observed at 1644 and 1562 cm^{-1} , respectively, in the FTIR spectra (Figure 4b). This shift in FTIR spectra suggests different structural conformations of the packed peptides on GNPs compared to the free peptides. Differential CD and FTIR spectra of CF Δ FNN clearly suggest conformational rearrangement of CF Δ FNN upon capping on GNPs. Similar results were also observed by Mandal et al. where secondary structure of free peptides differ from that present on GNP surface depending on nanoparticle curvature.⁴³

3.3. Peptide-Capped GNPs Can Entrap Small Drug Molecules. To further develop peptide-capped GNPs as drug delivery vehicles, we tested the ability of these nanoparticles to entrap small drug molecules. This noncovalent encapsulation of drugs onto GNP monolayer would provide direct release of unmodified drugs. Since core of these self-assembled monolayers (SAM) are hydrophobic, small hydrophobic drug like molecules should be well packed. To test the ability of CF Δ FNN-capped GNPs to entrap drugs, we used two anticancer drugs (Doxorubicin and Mitoxantrone), and one antimalarial drug (Chloroquine). All three drugs were loaded effectively by CF Δ FNN-capped GNPs. 55% of entrapment efficiency was observed with chloroquine, whereas 95% efficiency was observed in case of doxorubicin and mitoxantrone (Figure 5). CALNN-GNPs were taken as control and it showed entrapment efficiency of 45, 85, and 83% for chloroquine, doxorubicin and mitoxantrone respectively (Figure 5). Similar strategies have been taken to entrap and deliver hydrophobic drugs^{44,45} as radial character of monolayer creates hydrophobic pockets within the layer, which helps in efficient encapsulation of hydrophobic drugs and dyes.^{41,46–48}

3.4. Peptide-Capped GNPs Are Noncytotoxic. Noncytotoxicity of nanoparticles to mammalian cells is a prerequisite for drug delivery agents. To investigate whether the peptide-capped GNPs would have any toxic effects, we incubated two mammalian cell lines (HeLa and L929) and BALB/c mice spleenocytes with various concentrations of CALNN/CF Δ FNN capped GNPs for 24 and 72 h. The cytotoxicity of peptide capped

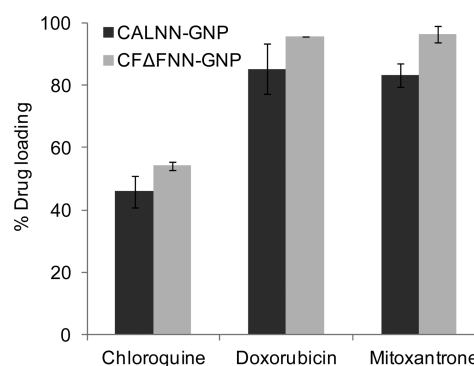


Figure 5. Entrapment of small drug molecules by CALNN/CF Δ FNN-capped GNPs. CF Δ FNN-capped GNPs showed enhanced entrapment efficiency than CALNN capped GNPs (mean \pm SD; $n = 3$).

GNPs was accessed by MTT assay. The relative viability of cells with different concentration of peptide capped GNPs was checked spectrophotometrically. The cell viability of peptide-GNPs treated samples were comparable to untreated control cells (Figure 6). Moreover, even at a very high concentration of 2 μM of peptide-capped GNPs, no toxic effect on cells was observed after treatment for 24 h as well as 72 h. Here PEI, CALNN, and CF Δ FNN were taken as controls. Peptide alone as well as peptide-capped GNPs showed no cytotoxicity, and viability was comparable to that of untreated cells.

3.5. Peptide-Capped GNPs Could Efficiently Transport Drugs to Mammalian Cells. GNPs of 20 nm are known to be taken up efficiently by mammalian cells.⁴⁹ However, surface modifications play important role in cellular uptake^{50–53} as well as function of GNPs.^{36,54} To study cellular uptake, Dox was taken as cargo drug for visualization under confocal microscopy. HeLa cells were incubated for 1 h with Dox, Dox + CF Δ FNN, and Dox + CF Δ FNN GNPs, and observed by microscopy. As shown in Figure 7, Dox in the absence and presence of peptide-capped GNPs was taken up by cells and characteristic nuclear localization of Dox could be observed.

Further evidence of cellular uptake of Dox in absence and presence of peptide capped GNPs was obtained by Fluorescence activated cell sorting (FACS) analysis. Dox entrapment in peptide capped GNPs was carried as described earlier. HeLa and L929 cells were incubated for 1 h with Dox (5 μM) in absence or presence of CALNN/CF Δ FNN-capped GNP. Interestingly, the

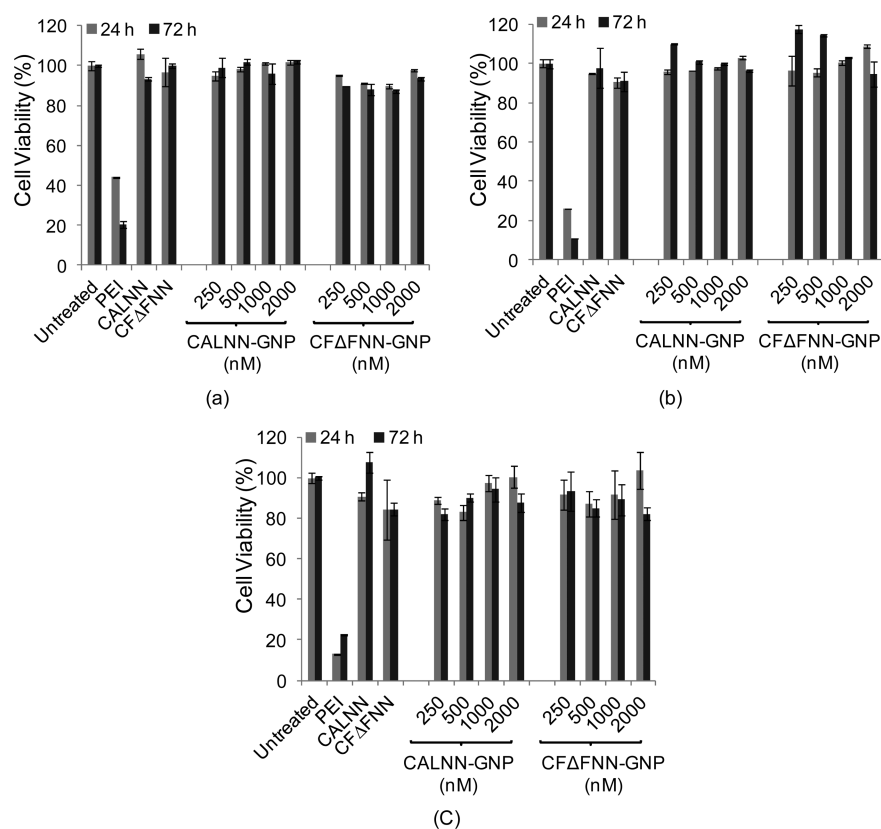


Figure 6. Cellular viability of (a) HeLa (b) L929 cells and (c) spleenocytes after treatment with peptide capped GNPs for 24 and 72 h measured by MTT assay. No cytotoxic effect observed after treatment with CALNN/CFΔFNN-capped GNPs (mean \pm SD; $n = 3$).

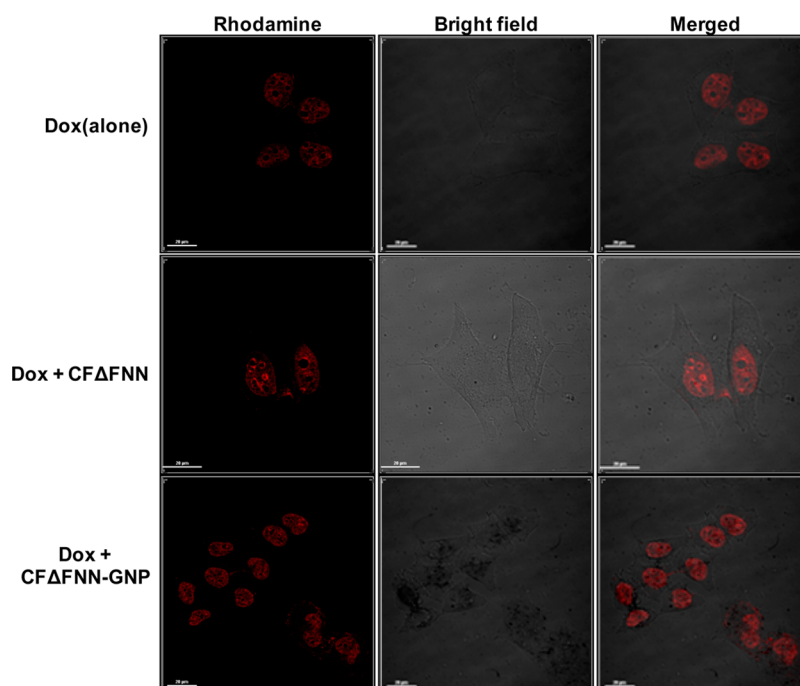


Figure 7. Confocal microscopy images of Dox ($5 \mu\text{M}$) uptake in HeLa cells with CFΔFNN ($5 \mu\text{M}$) or CFΔFNN-GNP (5 nM). Cells treated with Dox for 1 h (scale bar $20 \mu\text{m}$). Red represents fluorescence of Dox.

cellular uptake of Dox with CFΔFNN-GNP was 1.5 fold higher than Dox alone and when presented with CALNN-GNP in HeLa cells (Figure 8a). However, In L929 cells no such enhanced uptake of Dox in the presence of nanoparticles could be observed (Figure 8b).

3.6. CFΔFNN is Proteolytically More Stable than CALNN. To test whether the introduction of ΔPhe in the peptide affects the proteolytic stability of the modified pentapeptide, CFΔFNN and CALNN (native control peptide) was treated with nonspecific protease, proteinase K. Not surprisingly, CALNN was

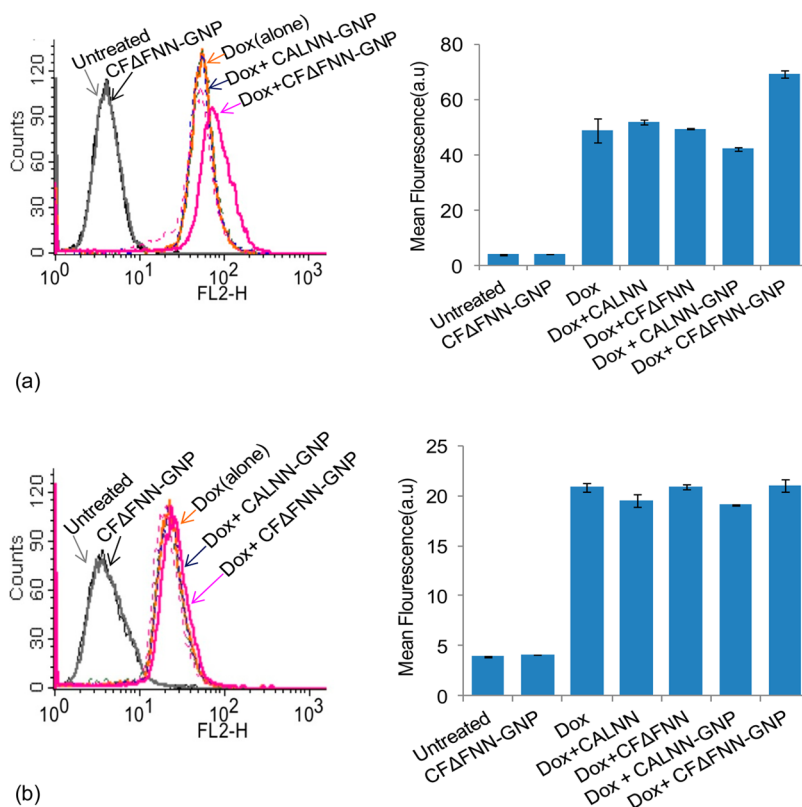


Figure 8. Flow cytometric data in (a) HeLa and (b) L929 cells for cellular uptake of Dox alone ($5 \mu\text{M}$) and in the presence of CFΔFNN, CALNN-GNP, and CFΔFNN-GNP for 1 h (mean \pm SD; $n = 3$).

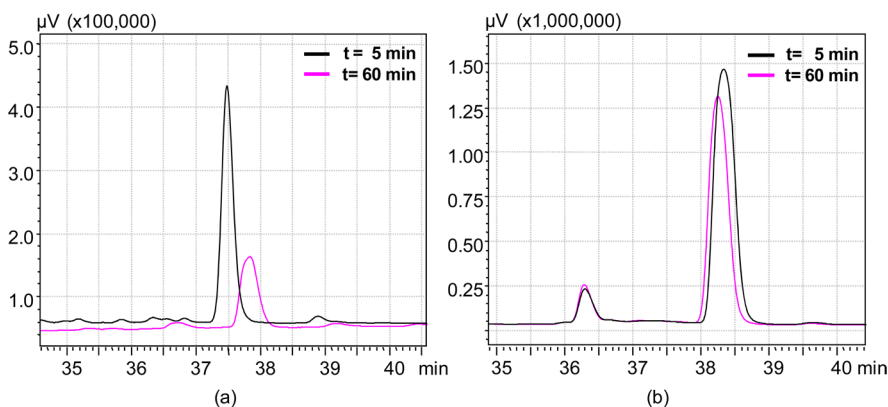


Figure 9. Protease stability of (a) CALNN and (b) CFΔFNN after proteinase K treatment for 1 hr. CFΔFNN showed enhanced proteolytic stability as compared to native peptide CALNN.

found to be susceptible to the action of proteinase K. After incubation at room temperature for 1 h, both CFΔFNN and CALNN were analyzed for degradation by HPLC. Peak intensity of CALNN peak was reduced by $\sim 55\%$ of initial peak intensity whereas CFΔFNN peak intensity was reduced by only $\sim 15\%$ (Figure 9). This is consistent with the earlier studies where ΔPhe incorporation in peptides is associated with its enhanced stability toward proteolysis.^{28,29}

3.7. CFΔFNN-GNP Effectively Delivers Drugs to Mammalian Cells. To assess the ability of CFΔFNN capped GNPs for delivery applications, we used two well-known anticancerous drugs [doxorubicin (Dox) and mitoxantrone (Mito)]. HeLa and L929 cells were incubated with native drug, drug + peptide, and drug + peptide-GNPs for 24 h, and their viability was determined using MTT assay. We used CALNN

and CALNN-capped GNPs as control for comparison. As shown in Figure 10a, percent viability of HeLa cells treated with free Dox ($5 \mu\text{M}$) was 31% and was comparable to that when delivered with CALNN or CFΔFNN. Dox when delivered with CALNN-GNP showed slight enhancement of toxicity with % viability of 27%. There was further enhancement in cytotoxicity of Dox when delivered with CFΔFNN-GNPs with 22% relative cell viability. Similar results were obtained when HeLa cells were treated with Mito (Figure 10 c). Forty-one percent cell viability was observed with free Mito ($10 \mu\text{M}$), which reduced to 28% when treated with CALNN-GNP. Mito with CFΔFNN-GNP showed highest cytotoxic effect with 19% cell viability. Figure 10b shows the cytotoxicity of L929 cells treated with Dox where comparable cell viability was observed in absence or presence of GNPs. However, L929 cells when treated with Mito enhanced

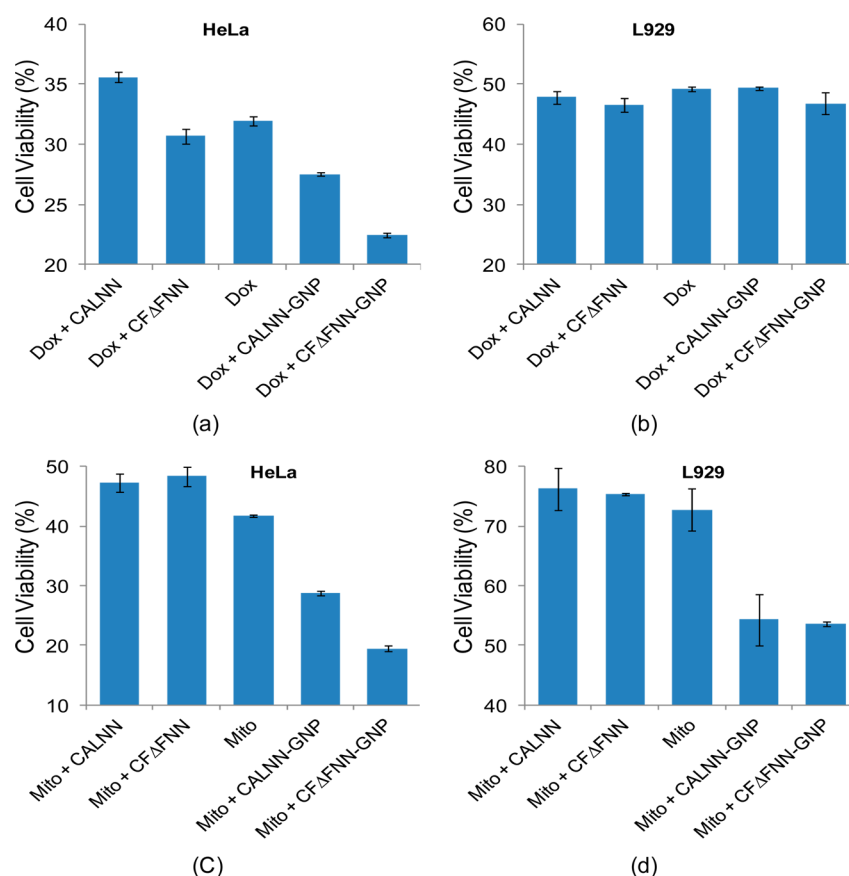


Figure 10. Cellular viability of (a, c) HeLa cells and (b, d) L929 cells on treatment with Dox ($5 \mu\text{M}$) and Mito ($10 \mu\text{M}$) in the absence or presence of peptide capped GNPs (mean \pm SD; $n = 3$).

cytotoxicity was observed when delivered with CFΔFNN-GNP. Here the cell viability changed from 71% with free mito treatment to 53% when mito was entrapped in CFΔFNN-GNP (Figure 10d). These results suggest that administration of Dox/Mito with CFΔFNN capped GNPs was more effective in killing HeLa cells as compared to free drug. Similar enhancement of anticancerous activity of drug has been observed when conjugated to GNPs.^{41,55,56}

4. CONCLUSION

In this work, we have shown that non-natural amino acids such as α,β -dehydrophenylalanine (ΔPhe) and α -aminobutyric acid (Aib) can be used in designing efficient capping agents for GNPs. Peptide-induced aggregation was not observed and some peptide capped GNPs were stable against salt induced aggregation. Peptide-capped GNPs were further characterized by TEM where 2 nm peptide layer was observed. Moreover, peptide-capped GNPs showed minimal cytotoxicity and efficiently entrapped small hydrophobic drugs like Doxorubicin, Mitoxantrone and Chloroquine. The cytotoxicity of drugs entrapped in peptide capped GNPs to HeLa cells was higher than the free drugs. These results indicate that non-natural amino acids containing peptide-capped GNPs could be promising drug delivery vehicles. Thus, this study opens a new avenue for designing a diverse array of peptide-capping agents for GNPs and further developing them as drug delivery agents.

■ AUTHOR INFORMATION

Corresponding Author

*Mailing address: International Centre for Genetic Engineering and Biotechnology, Aruna Asaf Ali Marg, New Delhi 110067,

India. Phone: 91-11-26742317. Fax: 91-11-26742316. E-mail: virander@icgeb.res.in.

Notes

The authors declare no competing financial interest.

■ ACKNOWLEDGMENTS

S.P. is thankful to University Grants Commission (UGC), India, for the award of Junior and Senior Research Fellowships. Core funding from ICGEB, New Delhi, and the Department of Biotechnology (DBT), India, are also acknowledged for this work. The authors thank Dr. Aseem Mishra for helping with electron microscopy. We acknowledge Mrs. Rashmi Shrivastava and Ankur Vashney for mass spectrometry analysis.

■ REFERENCES

- Jennings, T.; Strouse, G. *Adv. Exp. Med. Biol.* **2007**, *620*, 34–47.
- Uehara, N. *Anal. Sci.* **2010**, *26*, 1219–1228.
- Daniel, M. C.; Astruc, D. *Chem. Rev.* **2004**, *104*, 293–346.
- Jain, P. K.; Lee, K. S.; El-Sayed, I. H.; El-Sayed, M. A. J. *Phys. Chem. B* **2006**, *110*, 7238–7248.
- Kneipp, J.; Kneipp, H.; Rice, W. L.; Kneipp, K. *Anal. Chem.* **2005**, *77*, 2381–2385.
- Cobley, C. M.; Chen, J.; Cho, E. C.; Wang, L. V.; Xia, Y. *Chem. Soc. Rev.* **2011**, *40*, 44–56.
- Han, G.; Martin, C. T.; Rotello, V. M. *Chem. Biol. Drug Des.* **2006**, *67*, 78–82.
- Giljohann, D. A.; Seferos, D. S.; Daniel, W. L.; Massich, M. D.; Patel, P. C.; Mirkin, C. A. *Angew. Chem., Int. Ed.* **2010**, *49*, 3280–3294.
- Duchesne, L.; Gentili, D.; Comes-Franchini, M.; Fernig, D. G. *Langmuir* **2008**, *24*, 13572–13580.

- (10) Han, G.; Ghosh, P.; Rotello, V. M. *Nanomedicine* **2007**, *2*, 113–123.
- (11) Mulvaney, S. P.; Musick, M. D.; Keating, C. D.; Natan, M. J. *Langmuir* **2003**, *19*, 4784–4790.
- (12) Shan, J.; Tenhu, H. *Chem. Commun.* **2007**, 4580–4598.
- (13) Prasad, B. L. V.; Stoeva, S. I.; Sorensen, C. M.; Klabunde, K. J. *Langmuir* **2002**, *18*, 7515–7520.
- (14) Love, J. C.; Estroff, L. A.; Kriebel, J. K.; Nuzzo, R. G.; Whitesides, G. M. *Chem. Rev.* **2005**, *105*, 1103–1169.
- (15) Rana, S.; Bajaj, A.; Mout, R.; Rotello, V. M. *Adv. Drug Delivery Rev.* **2012**, *64*, 200–216.
- (16) Colombo, M.; Mazzucchelli, S.; Collico, V.; Avvakumova, S.; Pandolfi, L.; Corsi, F.; Porta, F.; Prosperi, D. *Angew. Chem., Int. Ed.* **2012**, *51*, 9272–9275.
- (17) Levy, R. *ChemBioChem* **2006**, *7*, 1141–1145.
- (18) Lévy, R.; Doty, R. C. Stabilization and Functionalization of Metallic Nanoparticles: the Peptide Route. In *Nanotechnologies for the Life Sciences*; Wiley-VCH: Weinheim, Germany, 2007.
- (19) Levy, R.; Thanh, N. T.; Doty, R. C.; Hussain, I.; Nichols, R. J.; Schiffrin, D. J.; Brust, M.; Fernig, D. G. *J. Am. Chem. Soc.* **2004**, *126*, 10076–10084.
- (20) Free, P.; Shaw, C. P.; Levy, R. *Chem. Commun.* **2009**, 5009–5011.
- (21) Maus, L.; Dick, O.; Bading, H.; Spatz, J. P.; Fiammengo, R. *ACS Nano* **2010**, *4*, 6617–6628.
- (22) Scari, G.; Porta, F.; Fascio, U.; Avvakumova, S.; Dal Santo, V.; De Simone, M.; Saviano, M.; Leone, M.; Del Gatto, A.; Pedone, C.; Zaccaro, L. *Bioconjugate Chem.* **2012**, *23*, 340–349.
- (23) Gentilucci, L.; De Marco, R.; Cerisoli, L. *Curr. Pharm. Des.* **2010**, *16*, 3185–3203.
- (24) See, V.; Free, P.; Cesbron, Y.; Nativo, P.; Shaheen, U.; Rigden, D. J.; Spiller, D. G.; Fernig, D. G.; White, M. R.; Prior, I. A.; Brust, M.; Lounis, B.; Levy, R. *ACS Nano* **2009**, *3*, 2461–2468.
- (25) Lien, S.; Lowman, H. B. *Trends Biotechnol.* **2003**, *21*, 556–562.
- (26) Mendel, D.; Ellman, J. A.; Chang, Z.; Veenstra, D. L.; Kollman, P. A.; Schultz, P. G. *Science* **1992**, *256*, 1798–1802.
- (27) Ma, J. S. *Chim. OGGI* **2003**, *21*, 65–68.
- (28) Gupta, M.; Chauhan, V. S. *Biopolymers* **2011**, *95*, 161–173.
- (29) Pathak, S.; Chauhan, V. S. *Antimicrob. Agents Chemother.* **2011**, *55*, 2178–2188.
- (30) Gupta, M.; Bagaria, A.; Mishra, A.; Mathur, P.; Basu, A.; Ramakumar, S.; Chauhan, V. S. *Adv. Mater.* **2007**, *19*, 858–861.
- (31) Kimling, J.; Maier, M.; Okenve, B.; Kotaidis, V.; Ballot, H.; Plech, A. *J. Phys. Chem. B* **2006**, *110*, 15700–15707.
- (32) Parween, S.; Gupta, P. K.; Chauhan, V. S. *Vaccine* **2011**, *29*, 2451–2460.
- (33) Kaiser, E.; Colescott, R. L.; Bossinger, C. D.; Cook, P. I. *Anal. Biochem.* **1970**, *34*, 595–598.
- (34) Mathur, P.; Ramakumar, S.; Chauhan, V. S. *Biopolymers* **2004**, *76*, 150–161.
- (35) Panda, J. J.; Mishra, A.; Basu, A.; Chauhan, V. S. *Biomacromolecules* **2008**, *9*, 2244–2250.
- (36) Olmedo, I.; Araya, E.; Sanz, F.; Medina, E.; Arbiol, J.; Toledo, P.; Alvarez-Lueje, A.; Giralt, E.; Kogan, M. J. *Bioconjugate Chem.* **2008**, *19*, 1154–1163.
- (37) Mishra, A.; Panda, J. J.; Basu, A.; Chauhan, V. S. *Langmuir* **2008**, *24*, 4571–4576.
- (38) Venkatpurwar, V.; Shiras, A.; Pokharkar, V. *Int. J. Pharm.* **2011**, *409*, 314–320.
- (39) Dhar, S.; Reddy, E. M.; Shiras, A.; Pokharkar, V.; Prasad, B. L. *Chem.—Eur. J.* **2008**, *14*, 10244–10250.
- (40) Mosmann, T. J. *Immunol. Methods* **1983**, *65*, 55–63.
- (41) Nasrolahi Shirazi, A.; Mandal, D.; Tiwari, R. K.; Guo, L.; Lu, W.; Parang, K. *Mol. Pharm.* **2013**, *10*, 500–511.
- (42) Kogan, M. J.; Olmedo, I.; Hosta, L.; Guerrero, A. R.; Cruz, L. J.; Albericio, F. *Nanomedicine* **2007**, *2*, 287–306.
- (43) Mandal, H. S.; Kraatz, H. B. *J. Am. Chem. Soc.* **2007**, *129*, 6356–6357.
- (44) Kim, C. K.; Ghosh, P.; Pagliuca, C.; Zhu, Z. J.; Menichetti, S.; Rotello, V. M. *J. Am. Chem. Soc.* **2009**, *131*, 1360–1361.
- (45) Duncan, B.; Kim, C.; Rotello, V. M. *J. Controlled Release* **2010**, *148*, 122–127.
- (46) Hostetler, M. J.; Stokes, J. J.; Murray, R. W. *Langmuir* **1996**, *12*, 3604–3612.
- (47) Lucarini, M.; Franchi, P.; Pedullì, G. F.; Pengo, P.; Scrimin, P.; Pasquato, L. *J. Am. Chem. Soc.* **2004**, *126*, 9326–9329.
- (48) Ghosh, P.; Han, G.; De, M.; Kim, C. K.; Rotello, V. M. *Adv. Drug Delivery Rev.* **2008**, *60*, 1307–1315.
- (49) Chithrani, B. D.; Ghazani, A. A.; Chan, W. C. *Nano Lett.* **2006**, *6*, 662–668.
- (50) Verma, A.; Uzun, O.; Hu, Y.; Han, H. S.; Watson, N.; Chen, S.; Irvine, D. J.; Stellacci, F. *Nat. Mater.* **2008**, *7*, 588–595.
- (51) de la Fuente, J. M.; Berry, C. C. *Bioconjugate Chem.* **2005**, *16*, 1176–1180.
- (52) Dhar, S.; Mali, V.; Bodhankar, S.; Shiras, A.; Prasad, B. L.; Pokharkar, V. *J. Appl. Toxicol.* **2011**, *31*, 411–420.
- (53) Morais, T.; Soares, M. E.; Duarte, J. A.; Soares, L.; Maia, S.; Gomes, P.; Pereira, E.; Fraga, S.; Carmo, H.; Bastos Mde, L. *Eur. J. Pharm. Biopharm.* **2012**, *80*, 185–193.
- (54) Moyano, D. F.; Goldsmith, M.; Solfiell, D. J.; Landesman-Milo, D.; Miranda, O. R.; Peer, D.; Rotello, V. M. *J. Am. Chem. Soc.* **2012**, *134*, 3965–3967.
- (55) Dhar, S.; Reddy, E. M.; Prabhune, A.; Pokharkar, V.; Shiras, A.; Prasad, B. L. *Nanoscale* **2011**, *3*, 575–580.
- (56) Hosta, L.; Pla-Roca, M.; Arbiol, J.; Lopez-Iglesias, C.; Samitier, J.; Cruz, L. J.; Kogan, M. J.; Albericio, F. *Bioconjugate Chem.* **2009**, *20*, 138–146.